

International Journal of Engineering Research and Development



DOI: 10.29137/ijerad.1684636

Volume:17 Issue:03 Pages:525-536 November/2025

Research Article

Enhancing Reliability of EV Charging Systems: Open-Circuit Fault Detection Using Advanced Signal Processing and Machine Learning

Hatice Okumuş* 10, Merve Mollahasanoğlu 10, Ebru Ergün 20

¹Department of Electrical and Electronics Engineering, Karadeniz Technical University, 61080 Trabzon, Türkiye ²Department of Electrical and Electronics Engineering, Recep Tayyip Erdogan University, 53100 Rize, Türkiye

Final Version: 30/11/2025

Abstract

As the use of electric vehicles (EVs) increases, the need for reliable and efficient power electronics in charging infrastructure is becoming increasingly critical. Such systems rely on switching elements such as IGBTs and SiC MOSFETs, which are prone to failure due to high operating temperatures and currents. As a solution to this problem this work proposes a new method for detecting open-circuit faults in AC/DC rectifiers used in EV charging stations. The proposed approach analyzes the three-phase current signals on the AC side to identify faulty switching elements. Feature extraction is performed using a hybrid method that combines the Discrete Wavelet Transform (DWT) and Teager-Kaiser Energy Operator (TKEO) techniques, which capture features related to transient faults. The extracted features are then classified using k-Nearest Neighbor (k-NN) and Random Forest (RF) algorithms. Performance evaluation is performed using 10-fold and 5-fold cross-validation methods. In both cases, RF yielded better results than k-NN in all metrics. As a result of 5-fold validation, RF achieved values of 0.9933, 0.9933, 0.9935, and 0.9933 for accuracy, precision, recall, and F1 score, respectively. These results validate the robustness and effectiveness of the RF-based method in fault detection, making it a promising tool for predictive maintenance and fault-tolerant electric vehicle charging systems.

Keywords

Electric vehicle, Power electronics Fault detection, Machine learning, k-Nearest neighbor, Random forest.

^{*} Corresponding Author: haticeokumus@ktu.edu.tr

1. Introduction

The need for sustainability and energy efficiency is causing an enormous disruption in the automotive sector currently. Concerns over the depletion of fossil fuels and global climate change have accelerated this shift with electric vehicles (EVs) garnering more attention due to their potential to improve energy efficiency and lessen their impact on the environment. EVs are becoming more and more popular in the industry because they have significant advantages over internal combustion engine (ICE) vehicles, including lower carbon emissions, increased energy efficiency and lower operating costs (Agrawal et al., 2020).

The critical role of power electronics systems which are essential parts that allow energy management and control in these vehicles has increased due to the widespread adoption of EVs. In order carry out critical functions like battery charging, motor drive operation and energy distribution overall, power electronics is essential to the conversion and regulation of electrical energy. The dependability and overall effectiveness of the system are directly impacted by important subsystems like battery management units, inverters, rectifiers, and DC-DC converters (Gopal et al., 2024). In these systems switching devices are especially important. Due to their superior performance, components like Silicon Carbide (SiC) Metal Oxide Semiconductor Field Effect Transistors (MOSFETs) and Insulated Gate Bipolar Transistors (IGBTs) are frequently utilized. Although SiC MOSFETs provide superior switching characteristics and exceptional thermal endurance, IGBTs are preferred in high-voltage applications due to their low conduction losses (Poolphaka et al., 2023). However, extended exposure to high temperatures, voltages, and currents increases the chance of device failure. These malfunctions jeopardize safety in addition to lowering system performance. Frequent electrical and thermal stress, especially when switching at high frequencies, can cause switching elements to gradually deteriorate and develop open- or short-circuit faults. Conventional methods, such as sensor-based monitoring, thermal analysis, and current-voltage waveform assessment, have been developed to identify such failures. Zhang et al. (2024) suggested a technique for detecting open-circuit faults in voltage source inverters using IGBT and SiC MOSFETs which is based on high-frequency oscillation current analysis. Results from experiments and simulations were used to validate their approach. Similarly, Ghosh et al. (2024) used statistical parameters like RMS, skewness and kurtosis derived from Discrete Wavelet Transform (DWT) coefficients to detect IGBT switching faults in three-level voltage source converters using a DWT based approach. Other research has suggested creative approaches. A fault diagnosis method for T-type rectifiers based on the proportion of fundamental to DC current components was presented by Wu et al. in 2023. By examining the average midpoint voltages of bridge legs, Song et al. (2024) created an affordable, sensorless technique for identifying open-circuit faults in NPC-DAB rectifiers. In order to find defective switches in Hybrid Active NPC rectifiers, Kim et al. (2020) used dq-axis analysis of three-phase currents. They validated their method through simulation and experimentation.

Artificial intelligence based methods are being used more and more for fault detection in power electronic systems as a result of advancements in computing and data processing. By using learning techniques they provide faster and more accurate diagnosis than traditional methods. In order to identify irregularities in the behavior of the system, facilitate predictive maintenance, reduce equipment downtime and prolong operational life, they thus analyze sizable data sets. As a result they lower maintenance costs and increase system reliability. For inverter systems fault diagnosis has emerged as a key area of study. In order to identify open-circuit faults in CHB inverters used in photovoltaic applications, Leon-Ruiz et al. (2024) suggested a two-stage fault classification method that combines signal processing and artificial neural networks. According to Parimalasundar et al. (2023), they employed Artificial Neural Networks (ANN) and Fast Fourier Transform (FFT) to detect open and short-circuit faults in H-bridge inverters. A multilayer perceptron (MLP) model was created by Sivapriya et al. (2023) to identify open circuit faults and it demonstrated a 96% accuracy rate on simulation and HIL platforms. Using an image-based approach, Du et al. (2021) claimed 100% classification accuracy by utilizing Deep Convolutional Neural Networks (DCNNs) like GoogLeNet and ResNet-50, Hilbert-Huang Transform (HHT), and Sparse Representation (SR). To identify issues with NPC inverters, Yuan et al. (2022) suggested a 1D CNN model with Improved Adamod (IAdamod) optimization. A deep learning model used by Liu et al. (2024) detected IGBT faults in three-phase inverters with 98.3% accuracy. Mestha et al. (2024) obtained a 99.92% accuracy rate by combining SVM optimized for SVOA with DTCWT based SqueezeNet. Methods of group learning have also proven successful. In order to achieve reliable diagnostic results in both simulation and hardware tests, Ibem et al. (2023) suggested a fault detection method based on the mean RMS ratio of phase currents using ensemble bagged classifiers. Research has also been conducted on DC-DC converters. To find open-circuit faults in isolated converters, Gong et al. (2020) used a CNN model with Global Average Pooling. In order to diagnose issues in embedded converter systems, Liu et al. (2024) combined Bayesian optimization with Extreme Learning Machines (ELM) and SVM with success rates exceeding 90%. Ye et al. (2020) achieved over 99% accuracy in detecting open and short-circuit faults in power plant converters using Wavelet Packet Transform and LSTM, and they validated their findings using HIL testing. Malik et al. (2023) created a DCNN-based model in 2023 to identify converter faults and simulations showed 96.3% accuracy.

In the context of AC-DC rectifiers, which play a vital role in EV charging infrastructure, fast and accurate fault detection is essential. Qin et al. (2023) proposed a model using Variational Mode Decomposition (VMD) and Dual Channel Recurrent Neural Networks (DCRNN) for single-phase PWM rectifiers achieving 96.27% accuracy with real-time simulation data. Kou et al. (2020) introduced a Deep Feedforward Network (DFN) model based on transient feature analysis achieving 97.85% accuracy. Cai et al. (2022) validated a 1D ResNet approach for fault detection in DAB rectifiers using HIL testing. Xu et al. (2024) trained an LSTM based deep neural network using front-end rectifier input currents and back-end converter transformer currents achieving 96.36% accuracy in DC charging station diagnostics. In the same direction Chen et al. (2024) combined LightGBM with an enhanced S-transform to identify and categorize open-circuit faults in EV charging systems exhibiting excellent results in both simulation and hardware settings.

In this study a novel open circuit fault detection approach for the AC/DC rectifier in EV charge stations is proposed. The method relies on analyzing the AC side three-phase current signals to identify the faulty switching device within the rectifier. Feature extraction is performed using a combination of Discrete Wavelet Transform (DWT) and Teager-Kaiser Energy Operator (TKEO) which enables effective representation of transient behaviors associated with fault conditions. These features are then classified using k-Nearest Neighbor (k-NN) and Random Forest (RF) algorithms. The proposed approach provides a reliable and accurate solution for detecting open-circuit faults in power electronic converters and it offers potential applications in predictive maintenance and fault-tolerant control strategies.

Symbols and Abbreviations

EV	Electric Vehicles
IGBTs	Insulated Gate Bipolar Transistors
MOSFETs	Metal Oxide Semiconductor Field Effect Transistors
FFT	Fast Fourier Transform
ANN	Artificial Neural network
MLP	Multi-Layer Perceptron
k-NN	k-Nearest Neighbors
RF	Random Forest
DWT	Discrete Wavelet Transform
TKEO	Teager-Kaiser Energy Operator

2. EV Charging Station

In EV charging systems, converting the grid-side alternating current (AC) into a direct current (DC) suitable for battery charging is a critical operation. Typically, such systems consist of a front-end AC/DC rectifier followed by a DC/DC converter. The AC/DC rectifier is responsible for ensuring a regulated DC output with high power quality and unity power factor while the DC/DC stage provides galvanic isolation and adjusts the voltage level according to the battery's requirements.

In the specified EV charging system given in Figure 1, there is a three-phase, six-switch, two-level AC/DC rectifier followed by an eight-switch isolated DC/DC converter. The AC/DC converter is used for converting grid-side AC voltage to a regulated DC voltage with power factor correction, while the DC/DC converter is used to provide galvanic isolation and adjust the voltage level according to the battery charging requirements. This system has been simulated in the MATLAB/Simulink environment using the parameters given in Table 1.

The general operation of the EV charging system has been validated by the results obtained and presented in Figure 2. The output voltage of 800 V DC from the AC/DC converter, the input current of 125 A to the DC/DC stage, the two-level AC/DC input terminal voltage, and the grid voltage and current waveforms indicate that the system operates in synchronization for a 100 kW EV charging system. Here, the x-axis represents time, while the y-axis represents magnitude, given in units of volts (V) and amperes (A). The switching states of the isolated DAB (Dual Active Bridge) converter are controlled using sinusoidal pulse width modulation (SPWM).

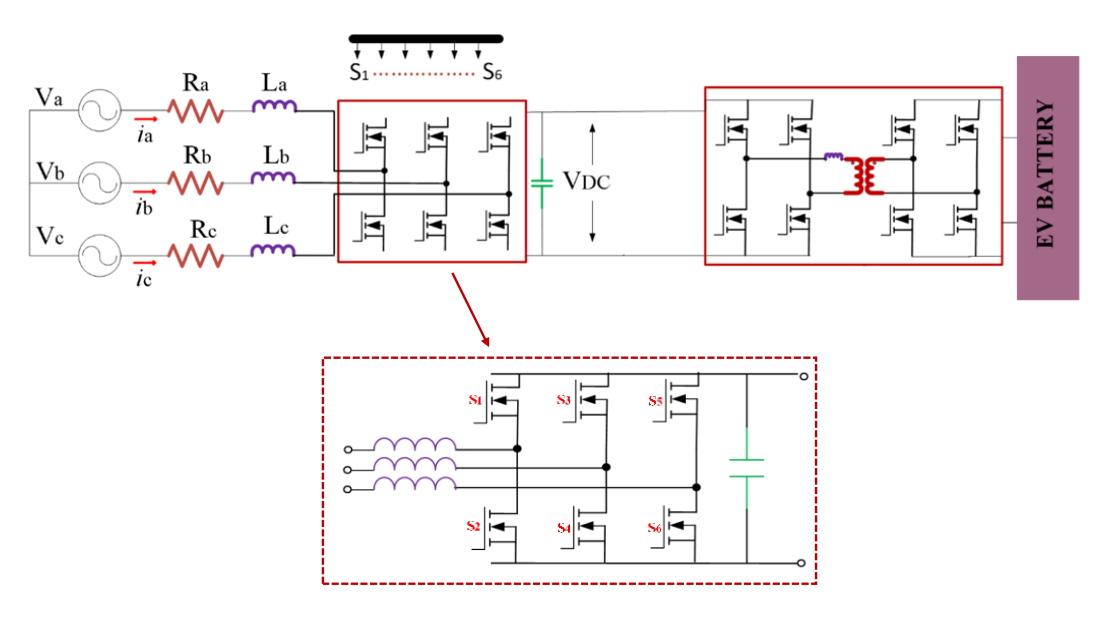


Figure 1. EV Charging Station.

This paper specifically concentrates on the detection of open-circuit faults occurring in the switching devices of the AC/DC rectifier, which is illustrated in detail in Figure 1.

Table 1.	Example	of Tables
----------	---------	-----------

Parameter	Value
Grid Voltage	400 V
Grid Frequency	50 Hz
Rectifier Output Voltage	800 V
Switching Frequency	1 kHz
Modulation Index	0.86
Input Impedance	1 mH
Input Resistance	0.01 Ω
Output Capacitors (C1 ve C2)	5200 μF
Rectifier Switches (C3M0060065D	V _{DSS} =650 V
– SiC MOSFET)	$R_{DS(on)}=60 \text{ m}\Omega$
	V_{SD} =4.8 V
Power Diodes (APT15D60B)	$V_R=600 V$
	$V_{F}=1.9 \text{ V}$
Control Parameters (Current-	$K_p = 0.02$
Voltage)	K _i =10.7
Control Parameter (DC side)	$K_p = 0.2$
	$K_i = 90$

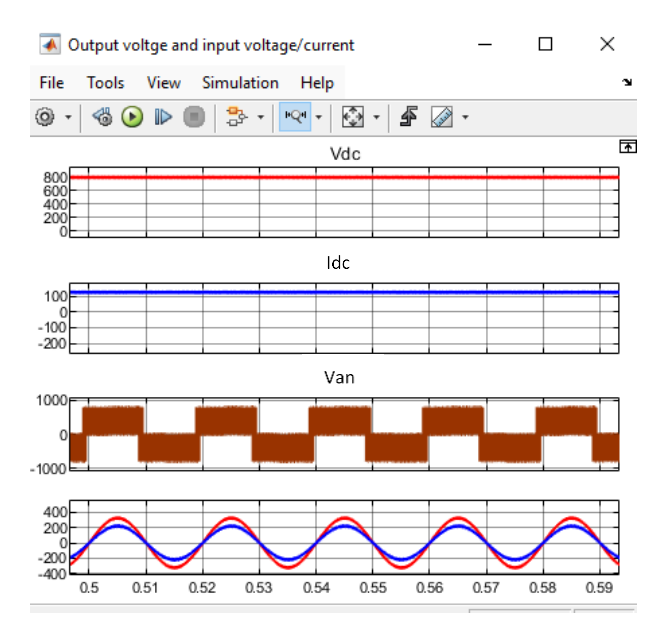


Figure 2. EV Charging System Outputs.

3. The Proposed Fault Classification Method

In this study, a fault detection model given in Figure 3 is proposed to identify the switching device with an open-circuit fault on the AC/DC rectifier. The methodology consists of three main stages: signal acquisition, feature extraction, and classification. Initially the three-phase AC current signals are collected from the AC side of the AC/DC rectifier model. In the second stage a hybrid signal processing approach combining Discrete Wavelet Transform (DWT) and the Teager–Kaiser Energy Operator (TKEO) is employed to extract discriminative features from the current waveforms. This combination enables capturing both time-frequency characteristics and nonlinear energy variations in the signals, which are highly indicative of fault signatures. In the final stage machine learning classifiers—k-Nearest Neighbors (k-NN) and Random Forest (RF)—are utilized to detect the faulty switching device.

The focus of this study is solely on the detection of open-circuit faults that may occur in the switching devices of the three-phase, six-switch, two-level AC/DC rectifier. For this purpose, the proposed method introduces open-circuit faults one at a time in the MOSFET

switching elements of the AC/DC rectifier within the EV charging system. Subsequently, three-phase AC input current signals are recorded with a 2 MHz sampling frequency over a duration of 1 second during each open circuit event. Open circuit are applied by removing the gate drive signal to the switch.

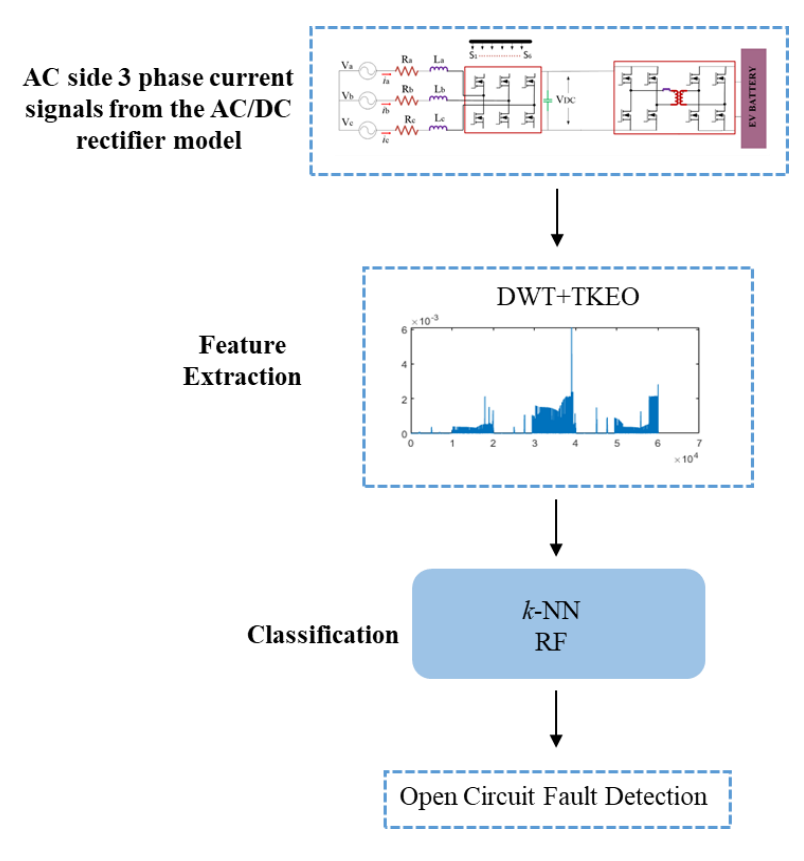


Figure 3. The Proposed Fault Detection Model

The effects of open-circuit faults occurring in switches S1 and S2, as well as the normal operating condition of the AC/DC rectifier, on the three-phase current signals measured from the grid side, are presented in Figure 4. Figure 4(a) shows the three-phase current waveforms under normal operating conditions of the rectifier. The currents here are observed to be sinusoidal and evenly distributed among the phases. Figures 4(b) and 4(c) illustrate the current waveforms under open-circuit fault conditions in switches S1 and S2, respectively. Due to the open-circuit fault, distortions occur in the phase to which the faulty switch is connected; the current waveforms become distorted, and some abrupt variations can be observed. In particular, interruptions in the current and loss of balance among the phases are notable. These distortions manifest as sudden changes during zero-crossings, asymmetries at peak points, and fluctuations in current amplitude. While the phase connected to the faulty switch is directly affected, the other phase currents are also indirectly influenced leading to an overall imbalance in the system.

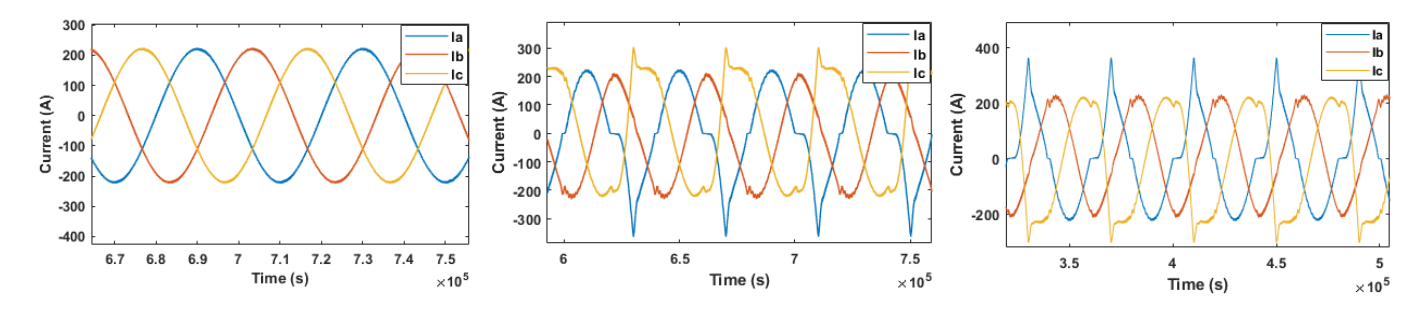


Figure 4. Three-phase Current Waveforms of The AC/DC Rectifier Under Normal and Open-circuit Fault Conditions.

3.1. Feature extraction

In this study a windowing technique was employed to facilitate the analysis of long-duration current signals and to effectively capture their characteristics within specific time intervals. Each raw signal was recorded for 1 second at a sampling rate of 2MHz resulting in

a total of 2000000 data points per signal. Processing the entire signal as a whole would be computationally intensive and inefficient for modeling purposes. To address this, the signals were segmented into fixed-length windows to create more manageable data structures. Given the sampling rate and the total number of data points, each signal was divided into 50 segments of 40000 data points.

As a result, the dimensionality of each signal was transformed into a matrix of size 50×40000. For six open-circuit fault cases, this process resulted in a combined dataset of size 300×40000. This method enables the segmentation of the time series into predefined window lengths allowing meaningful feature extraction from each segment. Following this process each segment undergoes wavelet decomposition and then the Teager-Kaiser Energy Operator (TKEO) to extract effective features.

3.1.1. Wavelet decomposition

Wavelet decomposition is a powerful signal processing technique used in order to analyze signals at multiple resolutions. Unlike traditional Fourier-based methods, which only provide frequency information, wavelet analysis retains both time and frequency localization. This is particularly advantageous for analyzing non-stationary signals where transient features play a critical role (Geng et al., 2025). For a signal x(t), the DWT is mathematically defined as:

$$DWT(w,n) = \int_{-\infty}^{\infty} x(t) \psi_{m,n}(t) dt$$
 (1)

where: $\psi_{m,n}(t)$ is the scaled and shifted version of the mother wavelet, m = scale parameter (related to frequency), n = translation (shift) parameter (related to time)

In the context of this study, DWT was employed to decompose the input current signals into various sub-bands capturing both coarse and detailed structures. The wavelet decomposition was implemented in MATLAB using the *wavedec* function with the Daubechies-18 (db18) mother wavelet. By repeatedly applying the decomposition, the signal were broken down into approximation and detail coefficients. The first-level detail coefficients obtained from the wavelet decomposition were processed using the TKEO to extract meaningful features from the signal. The filter length and boundary conditions were set to the default values in MATLAB's Wavelet Toolbox ensuring reproducibility. No additional normalization was applied during the feature extraction stage.

3.1.2. Teager-kaiser energy operator (TKEO)

The Teager-Kaiser Energy Operator (TKEO) is a nonlinear operator used to estimate the instantaneous energy of a signal by taking into account both its amplitude and frequency components. While classical energy calculations are typically based solely on the squared amplitude, TKEO offers a more sensitive measure capable of detecting abrupt variations in time-series data. For a discrete-time signal x[n], the TKEO is mathematically defined as;

$$\Psi[x[n]] = x[n]^2 - x[n+1].x[n-1]$$
 (2)

TKEO is frequently employed in applications that require the detection of transient events, such as speech processing, biomedical signal analysis, and fault diagnosis in electrical systems (Yu and Caspary, 2025). By highlighting localized energy bursts within a signal, the operator enhances feature extraction in nonstationary signal analysis.

3.2. Classification

3.2.1. k-Nearest neighbors (k-NN)

The k-Nearest Neighbor (k-NN) algorithm is a supervised machine learning approach widely used in classification tasks. Label assignment to test samples is done based on the classifications of their nearest neighbors in the training dataset. The algorithm works by evaluating the similarity or distance between data points in the training and test sets (Fazli & Poshtan, 2024). Various distance metrics such as Euclidean, Manhattan, Minkowski and Hamming can be used to determine proximity. In this study, the Euclidean distance (d) was employed, where the distance between two points m and r in an n-dimensional space is calculated as given in Eq. (3).

$$d = \sqrt{\sum_{i=1}^{n} (m_i - r_i)^2}$$
 (3)

A key factor influencing k-NN's performance is the choice of the parameter k, which defines how many neighbors will be considered during classification. Selecting an appropriate k value is crucial, as it directly impacts classification accuracy. In this study the number of neighbors (k) was set to 5.

3.2.2. Random forest (RF)

The Random Forest (RF) algorithm is constructed by combining multiple decision trees and aims to improve the generalization capability of the model by eliminating the weaknesses of individual trees.

The algorithm operates according to the following principles:

- Multiple subsets of the training data are created using random sampling with replacement (bootstrapping).
- An independent decision tree is trained on each subset. During the construction of each tree, a random subset of features is selected at each node to determine the best split. This strategy enhances model diversity and reduces the risk of overfitting.
- In classification problems, the final prediction is determined through majority voting, where each tree contributes one vote for a class label. In regression problems, the final output is obtained by averaging the predictions of all trees.

The Random Forest algorithm offers several advantages, including high accuracy, robustness against overfitting, and the ability to handle missing data (Gohari and Ghorbani, 2025). In this study, for RF classifier, MATLAB's TreeBagger implementation was used with 100 trees, while other parameters (such as maximum depth, split criterion, and feature selection strategy) were kept at their default values.

3.2.3. Performance metrics

To conduct a detailed assessment of the proposed classification model's performance, four commonly used performance metrics were employed: accuracy, precision, recall, and F1-score. These metrics provide a balanced evaluation by considering both the overall correctness and the class-wise performance of the model.

Let TP (true positives) denote the number of correctly identified positive instances, TN (true negatives) the number of correctly identified negative instances, FP (false positives) the number of negative cases incorrectly classified as positive, and FN (false negatives) the number of positive cases incorrectly classified as negative.

Accuracy reflects the proportion of correctly classified instances among the total number of instances as given in Eq.(4), offering a general measure of model performance.

$$Accuracy = \frac{TP + TN}{TP + TN + FP + FN} \tag{4}$$

Precision indicates the proportion of correctly predicted positive observations to the total predicted positives as in Eq.(5), thus emphasizing the model's ability to avoid false positives.

$$Precision = \frac{TP}{TP + FP} \tag{5}$$

Recall (also known as sensitivity) calculated as in Eq.(6) represents the proportion of actual positive observations that were correctly identified, measuring the model's capacity to capture relevant instances.

$$Recall = \frac{TP}{TP + FN} \tag{6}$$

F1-score is the harmonic mean of precision and recall given as in Eq.(7), and it provides a single metric that balances both false positives and false negatives.

$$F1 - score = 2.\frac{Precision.Recall}{Precision+Recall}$$
 (7)

In this study, for precision, recall, and F1-score, macro-averaging was used where the metrics were first calculated independently for each class, and then their mean was taken to obtain the final scores. This approach ensures that all classes contribute equally to the overall performance evaluation, regardless of their frequency in the dataset. The average accuracy was calculated as the sum of the diagonal elements of the confusion matrix divided by the total number of instances.

4. Results and Discussion

In this study 5-fold and 10-fold cross-validation methods were employed to evaluate the accuracy and generalizability of the model. Cross-validation is a widely used model validation technique to prevent overfitting to the training data and to objectively assess the model's performance on different subsets of the data. In the k-fold cross-validation method, the dataset is split into k subsets of equal size. In each iteration, one of these subsets is used as the test set while the remaining k-1 subsets are used for training. This process is repeated k times with each subset used once as the test set. In this paper, the switches are denoted as S1–S6 as mentioned before, and for classification purposes, the open-circuit fault occurring in each switch is referred to as class OCF-S1, OCF-S2, ... OCF-S6, respectively.

In the 5-fold cross-validation results presented in Table 2 both k-NN and RF classifiers demonstrate strong classification performance across all six classes (OCF-S1 to OCF-S6). The overall accuracy ranges from 0.9867 to 1.0000 suggesting minimal misclassification and a high level of class separability. For the k-NN classifier, precision and recall are generally above 0.9800 for all classes except for OCF-S1 where the precision drops to 0.9259. This indicates that k-NN produced some false positives for OCF-S1, although its recall remains perfect (1.000), meaning all true instances were correctly identified. The resulting F1-score for OCF-S1 is 0.9615 while the scores for other classes exceed 0.9800 highlighting the model's overall robustness. The RF classifier shows even more consistent results. Precision and recall scores are nearly perfect across all classes, with F1-scores of 1.0000 achieved for OCF-S3 and OCF-S5, indicating flawless performance. Slight declines in precision for OCF-S4 (0.9804) and OCF-S6 (0.9804) point to a small number of false positives, yet the F1-scores for these classes remain above 0.9901.Comparatively, RF outperforms k-NN in terms of precision, particularly for classes like OCF-S1 and OCF-S2 where k-NN shows minor instability. The consistently high F1-scores of RF across all classes suggest better generalization and reliability, especially in contexts where precision is a key evaluation metric.

Table 2. 5 Fold Cross-validation Results

Class _ Label		k-NN			RF			
	Accuracy	Precision	Recall	F1	Accuracy	Precision	Recall	F1
OCF-S1	0.9867	0.9259	1.0000	0.9615	0.9967	1.0000	0.9800	0.9899
OCF-S2	0.9933	0.9800	0.9800	0.9800	0.9967	1.0000	0.9800	0.9899
OCF-S3	0.9967	1.0000	0.9800	0.9899	1.0000	1.0000	1.0000	1.0000
OCF-S4	0.9967	1.0000	0.9800	0.9899	0.9967	0.9804	1.0000	0.9901
OCF-S5	0.9967	1.0000	0.9800	0.9899	1.0000	1.0000	1.0000	1.0000
OCF-S6	0.9967	1.0000	0.9800	0.9899	0.9967	0.9804	1.0000	0.9901

The 10-fold cross-validation results in Table 3 reinforce these findings. Both classifiers maintained high accuracies ranging from 98.00% to 100.00% across all classes (OCF-S1- OCF-S6), thus confirming their ability to effectively distinguish class labels even under increasing fold variability. While sensitivity remained high for k-NN across all classes, precision dropped again for OCF-S1 (0.9074) resulting in a lower F1-score for this class (0.9423). This reflects a higher false positive rate for OCF-S1 despite maintaining high sensitivity (recall = 0.9800). In the other classes k-NN achieved nearly perfect precision and sensitivity, with F1-scores very close to or equal to 0.9899. The RF classifier maintained its superior performance achieving perfect precision and sensitivity for OCF-S3 and OCF-S4, while achieving excellent F1-scores. In other classes such as OCF-S1, OCF-S2 and OCF-S5, sensitivity remained high with only minor decreases observed, resulting in F1-scores above 0.98 across all classes.

Overall, RF exhibits greater stability and predictive power than k-NN, particularly when addressing more challenging classes. Its consistent performance across both validation schemes demonstrates its suitability for applications where precision and generalization are critical.

Table 3. 10 Fold Cross-validation Results

		k-NN			RF			
Class _ Label	Accuracy	Precision	Recall	F1	Accuracy	Precision	Recall	F1
OCF-S1	0.9800	0.9074	0.9800	0.9423	0.9967	1.0000	0.9800	0.9899
OCF-S2	0.9933	0.9800	0.9800	0.9800	0.9933	0.9800	0.9800	0.9800
OCF-S3	0.9967	1.0000	0.9800	0.9899	1.0000	1.0000	1.0000	1.0000
OCF-S4	0.9967	1.0000	0.9800	0.9899	1.0000	1.0000	1.0000	1.0000
OCF-S5	0.9967	1.0000	0.9800	0.9899	0.9933	0.9800	0.9800	0.9800
OCF-S6	0.9967	1.0000	0.9800	0.9899	0.9967	0.9804	1.0000	0.9901

Table 4 presents the average performance metrics for both k-NN and RF classifiers under 5-fold and 10-fold cross-validation settings. When all metrics—accuracy, sensitivity, precision, and F1-score—are examined, it is seen that the RF classifier consistently outperforms k-NN in both validation strategies. Especially in 10-fold validation, RF reached accuracy and sensitivity values of 0.9900, while these values of k-NN remained at 0.9800. This result shows that RF not only makes more accurate predictions overall, but also

captures more true positives. Precision and F1-score follow the same trend; RF achieved values of 0.9901 and 0.9900, respectively, while k-NN produced slightly lower values (precision 0.9812 and F1-score 0.9803). A similar pattern was observed in the 5-fold validation, with RF again demonstrating superior performance. k-NN achieved an accuracy of 0.9833 and an F1-score of 0.9835, while RF achieved a value of 0.9933 in both metrics. The difference is particularly pronounced in precision values; RF achieved 0.9935, while k-NN remained at 0.9843, demonstrating that RF is more effective in reducing false positives. Additionally, Table 4 presents results obtained using only DWT features. Compared to the DWT+TKEO approach the overall performance is seen to decrease confirming the additional contribution of the TKEO feature set. Uder 10-fold cross-validation, the RF classifier achieves an accuracy of 0.9800 with DWT alone while this value reaches 0.9900 when used with TKEO. A similar trend is observed in the k-NN classifier where the accuracy value drops from 0.9800 to 0.9667. These results demonstrate that the integration of TKEO with DWT provides richer discriminative information and leads to superior classification performance. TKEO can therefore be viewed as an additional feature extraction technique that improves on conventional DWT-based representations.

These findings support the fact that the RF classifier is not only more accurate but also more stable across different validation settings. Higher precision and sensitivity values indicate a better balance between false positives and false negatives, making RF a more reliable option, particularly in applications where classification accuracy is critical.

Table 4. Average Performance Metric Values for Each Method

Metric		DWT+TKEO				DWT			
	10 Fold		5 Fold		10 Fold		5 Fold		
	k-NN	RF	k-NN	RF	k-NN	RF	k-NN	RF	
Acc	0.9800	0.9900	0.9833	0.9933	0.9667	0.9800	0.9700	0.9833	
Recall	0.9800	0.9900	0.9833	0.9933	0.9667	0.9800	0.9700	0.9833	
Prec	0.9812	0.9901	0.9843	0.9935	0.9695	0.9801	0.9722	0.9834	
F1	0.9803	0.9900	0.9835	0.9933	0.9672	0.9800	0.9705	0.9833	

Figures 5 and 6 present the average confusion matrices of the *k*-NN and RF classifiers under 5-fold and 10-fold cross-validation respectively. In the 5-fold scenario, the RF classifier demonstrates nearly perfect classification performance across all classes; values on the diagonal approach 10.0, while off-diagonal misclassifications remain extremely low. This demonstrates that the model effectively distinguishes all class labels, demonstrating high accuracy and consistent performance. In contrast, the k-NN classifier, while generally strong, exhibits minor errors in classes other than OCF-S1, with a small number of instances being incorrectly assigned to neighboring classes. Such subtle errors are consistent with the sensitivity of k-NN, particularly in classes with closely spaced feature areas.

A similar trend is observed in the 10-fold cross-validation results. The RF model maintains excellent classification accuracy in most classes, with only negligible misclassifications (e.g., 0.1 in OCF-S1, OCF-S2 and OCF-S5). The k-NN classifier still exhibits minor confusion, with some misassignments, particularly between OCF-S5 and OCF-S6, but its overall performance remains high. These results reinforce that RF offers more precise and reliable class separation even in multi-layered verification scenarios. The complexity matrices clearly demonstrate the robustness of the RF model and its ability to minimize both false positives and false negatives.

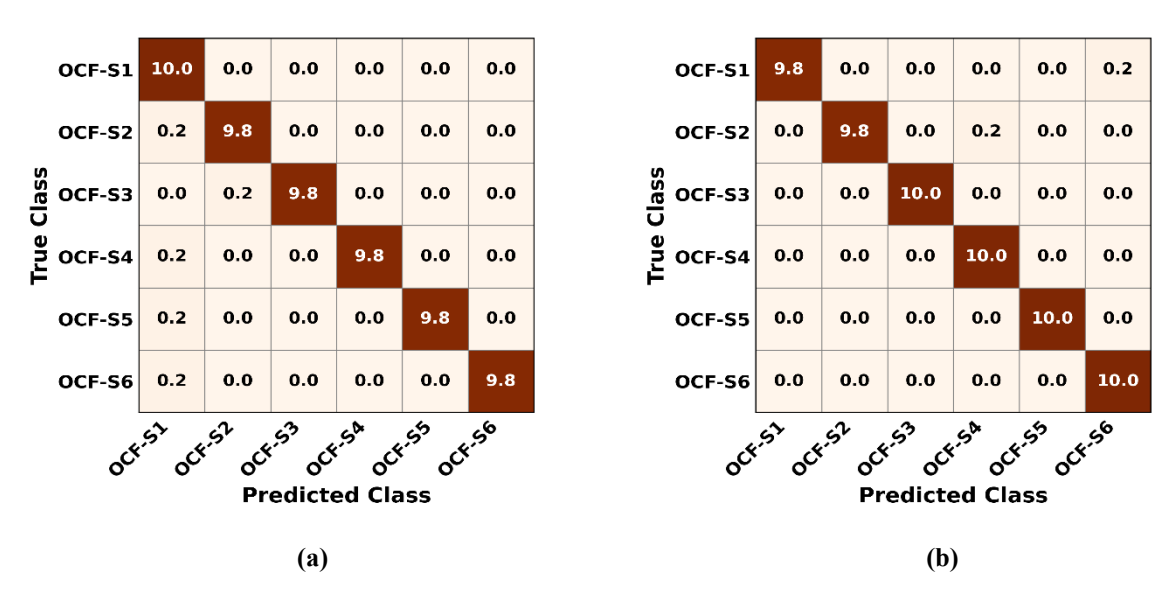
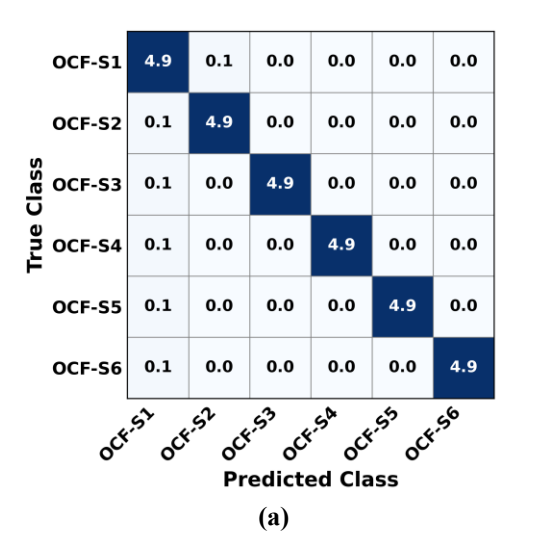


Figure 5. Average Confusion Matrixes for (a) k-NN; (b) RF for 5 Fold.



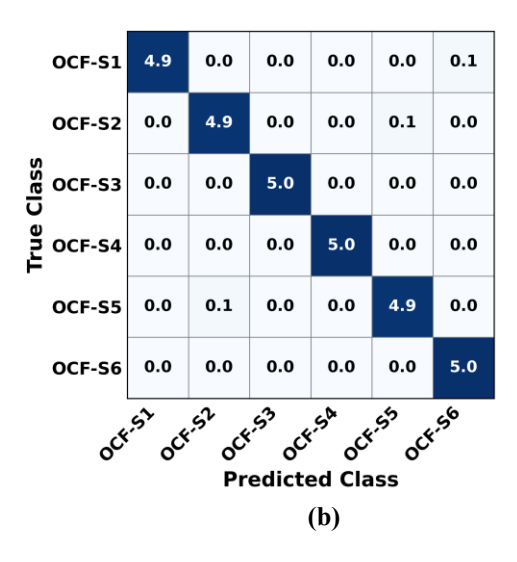


Figure 6. Average Confusion Matrixes for (a) k-NN; (b) RF for 10 Fold.

5. Conclusion

In this study, an effective open-circuit fault detection approach is proposed for the AC side of an AC/DC converter system. The method integrates signal processing and machine learning techniques by extracting meaningful features through the framework combining DWT and TKEO, then performs classification with k-NN and RF algorithms. Performance evaluations with 5-fold and 10-fold cross-validation showed that the proposed model gives very high accuracy results. In particular, the RF classifier achieved the highest performance in all metrics, achieving 99.33% accuracy in 5-fold validation and 99.00% accuracy in 10-fold validation. The high precision, sensitivity, and F1-score values further confirm the model's robustness and reliability in detecting open-circuit faults.

The strength of the proposed methodology lies in its hybrid feature extraction framework (DWT + TKEO) which effectively captures both time-frequency characteristics and instantaneous energy information. This enables even relatively simple and computationally efficient classifiers such as k-NN and RF to achieve superior results without requiring more complex models.

For future work the proposed model can be extended to detect other types of converter faults including short-circuit and intermittent faults. Additionally, real-time implementation on embedded systems or DSP platforms can be explored to validate the approach under practical operating conditions. Incorporating adaptive or deep learning-based classifiers may also enhance the model's generalization capability, especially in scenarios involving varying load and noise conditions.

References

Agrawal, M., Rajapatel, M. S. (2020). Global perspective on electric vehicle. International Journal of Engineering Research & Technology, 9(1), 8-11.

Cai, F., Zhan, M., Chai, Q., Jiang, J. (2022). Fault diagnosis of DAB converters based on ResNet with adaptive threshold denoising. IEEE Transactions on Instrumentation and Measurement, 71, 1-10.

Chen, Y., Tang, Z., Weng, X., He, M., Zhou, S., Liu, Z., Jin, T. (2024). A diagnostic method for open-circuit faults in DC charging stations based on improved S-transform and LightGBM. Energies, 17(2), 404.

Du, B., He, Y., Zhang, C. (2021). Intelligent diagnosis of cascaded H-bridge multilevel inverter combining sparse representation and deep convolutional neural networks. IET Power Electronics, 14(6), 1121-1137.

Fazli, A., Poshtan, J. (2024). Wind turbine fault detection and isolation robust against data imbalance using KNN. Energy Science & Engineering, 12(3), 1174-1186.

Geng, X., Wang, L., Yu, P., Hu, W., Liang, Q., Zhang, X., & Zhang, X. (2025). A method of EEG signal feature extraction based on hybrid DWT and EMD. Alexandria Engineering Journal, 113, 195-204.

Ghosh, S. S., Chattopadhyay, S., Das, A., Medikondu, N. R., Almawgani, A. H., Alhawari, A. R., Das, S. (2024). Wavelet-based rapid identification of IGBT switch breakdown in voltage source converter. Microelectronics Reliability, 152, 115283.

Gohari, M., & Ghorbani, M. H. (2025). Classification and diagnosis of the rotor unbalance parameters via hybridized EMD and RF. Journal of Vibration Engineering & Technologies, 13(4), 246.

Gong, W., Chen, H., Zhang, Z., Zhang, M., & Gao, H. (2020). A data-driven-based fault diagnosis approach for electrical power DC-DC inverter by using modified convolutional neural network with global average pooling and 2-D feature image", IEEE Access, 8, 73677-73697.

Gopal, S. D., Jawahar, R., Athmanathan, R., Pandi, M. (2024). Power electronics converters for an electric vehicle fast charging station based energy storage system and renewable energy sources: Hybrid approach. Optimal Control Applications and Methods, 45(2), 646-673.

Ibem, C. N., Farrag, M. E., Aboushady, A. A., Dabour, S. M. (2023). Multiple open switch fault diagnosis of three phase voltage source inverter using ensemble bagged tree machine learning technique. IEEE Access, 11, 85865-85877.

Kim, S. H., Kim, S. M., Park, S., Lee, K. B. (2020). Switch open-fault detection for a three-phase hybrid active neutral-point-clamped rectifier. Electronics, 9(9), 1437.

Kou, L., Liu, C., Cai, G. W., Zhang, Z., Zhou, J. N., Wang, X. M. (2020). Fault diagnosis for three-phase PWM rectifier based on deep feedforward network with transient synthetic features. ISA transactions, 101, 399-407.

León-Ruiz, Y., González-García, M., Alvarez-Salas, R., Cárdenas, V., Diaz, R. I. V. (2024). Fault diagnosis in a photovoltaic grid-tied CHB multilevel inverter based on a hybrid machine learning and signal processing technique. IEEE Access.

Liu, Y., Sangwongwanich, A., Zhang, Y., Ou, S., & Wang, H. (2024, February). A Transferable Deep Learning Network for IGBT Open-circuit Fault Diagnosis in Three-phase Inverters. In 2024 IEEE Applied Power Electronics Conference and Exposition (APEC) (pp. 1229-1234).

Liu, Y., Zhang, G., Miao, J., Zhao, Z., Yin, Q., Zhao, J. (2024). Fault Diagnosis of DC/DC Buck Converter for Embedded Applications Based on BO-ELM. IEEE Transactions on Industrial Electronics.

Malik, J. A., Haque, A., & Amir, M. (2023, May). Investigation of intelligent deep convolution neural network for DC-DC converters faults detection in electric vehicles applications. In 2023 International Conference on Recent Advances in Electrical, Electronics & Digital Healthcare Technologies (REEDCON) (pp. 139-144).

Mestha, S. R., Prabhu, N. (2024). Support vector machine based fault detection in inverter-fed electric vehicle. Energy Storage, 6(1), e576.

Parimalasundar, E., Kumar, R. S., Chandrika, V. S., Suresh, K. (2023). Fault diagnosis in a five-level multilevel inverter using an artificial neural network approach. Electrical Engineering & Electromechanics, (1), 31-39.

Poolphaka, P., Jamshidpour, E., Lubin, T., Baghli, L., Takorabet, N. (2023). Comparative study of IGBT and SiC MOSFET three-phase inverter: Impact of parasitic capacitance on the output voltage distortion. In Actuators 12(9), 355.

Qin, N., Wang, T., Huang, D., You, Y., Zhang, Y. (2023). VWM-DCRNN: A method of combining signal processing with deep learning for fault diagnosis in single-phase PWM rectifier. IEEE Transactions on Power Electronics, 38(7), 8894-8906.

Sivapriya, A., Kalaiarasi, N., Vishnuram, P., Abou Houran, M., Bajaj, M., Pushkarna, M., Kamel, S. (2023). Real-time hardware-in-loop based open circuit fault diagnosis and fault tolerant control approach for cascaded multilevel inverter using artificial neural network. Frontiers in Energy Research, 10, 1083662.

Song, C., Sangwongwanich, A., Blaabjerg, F. (2024). Sensorless open-circuit-fault diagnosis method for NPC-based DAB converter. IEEE Transactions on Power Electronics, 39(9), 10699-10703.

Xu, Y., Zou, Z., Liu, Y., Zeng, Z., Zhou, S., Jin, T. (2024). Deep learning-based multi-feature fusion model for accurate open circuit fault diagnosis in electric vehicle DC charging piles. IEEE Transactions on Transportation Electrification, 11(1), 2243-2254.

Wu, Z., Zhao, J., Luo, H., Liu, Y. (2023). Real-time open-circuit fault diagnosis method for T-type rectifiers based on median current analysis. IEEE Transactions on Power Electronics, 38(7), 8956-8965.

Ye, S., Jiang, J., Li, J., Liu, Y., Zhou, Z., Liu, C. (2020). Fault diagnosis and tolerance control of five-level nested NPP converter using wavelet packet and LSTM. IEEE Transactions on Power Electronics, 35(2), 1907-1921.

Yu, X., & Caspary, O. (2025). TKEO-Enhanced Machine Learning for Classification of Bearing Faults in Predictive Maintenance. Applied Sciences (2076-3417), 15(7).

Yuan, W., Li, Z., He, Y., Cheng, R., Lu, L., Ruan, Y. (2022). Open-circuit fault diagnosis of NPC inverter based on improved 1-D CNN network. IEEE Transactions on Instrumentation and Measurement, 71, 1-11.

Zhang, J., Li, H., Xiang, D., & Lei, X. (2024). A fast and robust open-circuit fault detection method for voltage-source-inverter with integrated high-frequency sensor. IEEE Journal of Emerging and Selected Topics in Power Electronics.